33RD INTERNATIONAL COSMIC RAY CONFERENCE, RIO DE JANEIRO 2013
THE ASTROPARTICLE PHYSICS CONFERENCE

ICRC 2013

Direct Dark Matter Search with XMASS

MASAKI YAMASHITA[1,2], FOR THE XMASS COLLABORATION.

[1] *Kamioka Observatory, Institute for Cosmic Ray Research, the University of Tokyo*
[2] *Kavli Institute for the Physics and Mathematics of the Universe (WPI), the University of Tokyo*

yamashita@icrr.u-tokyo.ac.jp

Abstract: XMASS is a multi-purpose experiment which aims at the direct detection of dark matter, low energy solar neutrinos, and neutrino less double beta decay with a ton scale fiducial volume of liquid xenon detector. In the current stage, we focus on the the direct detection of dark matter in the form of WIMPs (Weakly Interacting Massive Particles) via their elastic scattering off xenon nuclei with 835 kg detector at Kamioka in Japan. The first result from a low mass WIMP search done with a very low energy threshold is presented.

Keywords: Dark Matter, WIMP, liquid xenon

1 Introduction

XMASS is a multi-purpose of ultra pure liquid xenon detector for the underground physics and its targets are dark matter search, low energy solar neutrinos and neutrinoless double beta decay with ton scale fiducial volume [1]. The current phase of XMASS is to use 835 kg liquid xenon detector mainly for the dark matter search as well as solar axion [2] prior to the second stage of 5 ton with 1ton fiducial volume detector (XMASS 1.5). Based on the results and experiences which will be obtained by those detectors, the final detector will be employed for the study of low energy solar neutrinos and the further investigation of dark matter. Substantial evidences that the universe is composed of dark matter have been reported [3] and Weakly Interacting Massive Particles (WIMPs) is the one of main candidate for the cold dark matter. WIMPs populating the halo of our galaxy can be detected directly via their interactions with nuclei in terrestrial detectors. In this article, the 5.6 ton·day exposure of data which was taken in February 2012 with very low energy threshold is shown. With these data and without discriminating between nuclear-recoil and electronic events XMASS excludes part of the WIMP-nucleon cross section and WIMP mass parameter space allowed by other measurements.

2 XMASS Detector

The XMASS detector was installed in the newly excavated experimental hall at Kamioka in Japan in 2010 and its detail design and performances are described in [4]. Fig.1 shows the water tank, ϕ 10 m $\times$ 10m, which is used for the radiation shield of neutrons and gamma rays from the rock. The vacuum insulated OFHC Copper detector vessel which holds the liquid xenon was installed in the middle of water tank. The detector employs a single phase technology and observes only scintillation lights emitted by the interaction of dark matter. The total amount of liquid xenon for active volume is about 835 kg and the total mass of liquid xenon in the detector is 1080 kg. The 642 hexagonal photomultiplier tubes (PMTs), R10789 Hamamatsu, are mounted in an approximately spherical shape with an average radius of 40 cm of xenon as shown in Fig. 2. PMTs photo-cathode give about 64.4% coverage of the inner surface of the detector.

The purification of xenon in gas phase is performed by

Fig. 1: Water tank for radiation shield against neutrons and gamma rays from the rock. The size is ϕ 10 m $\times$ H 10 m and the vacuum insulated OFHC Copper vessel which holds liquid xenon was mounted in the center.

SAES getter at the 30L/min of flow rate during the filling with two 200W pulse tube refrigerators. The recirculation of xenon in liquid phase is also possible at a few L/min (LXe) of flow rate for the purification ,if necessary.

3 Data and Event Selection

The data used for the analysis, corresponding to 6.70 days of live time, was taken from February, 21st to 28th in 2012. The detail data selection and calibration were described in [5]. PMT signals are amplified with a voltage gain factor of 11 before being processed by Analog-Timing-Modules (ATMs) [6]. These modules combine the functions of typical ADC and TDC modules, recording both the integrated charge and the arrival time of each PMT signal.

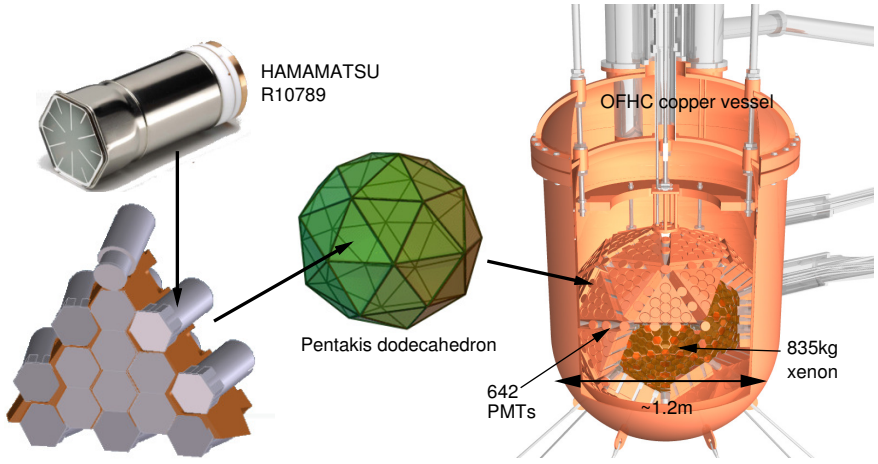

Fig. 2: Structure of PMT holder and the vacuum insulated OFHC Copper vessel.

For each PMT channel, the discriminator threshold is set to −5 mV, which corresponds to 0.2 photoelectrons (p.e.). When a PMT signal is above threshold a "hit" is registered on the module. A global trigger is generated based on the number of hit PMTs within a 200 ns window. The trigger threshold was required four PMT hits to achieve low energy threshold. Using 122 keV gamma rays from the ^{57}Co calibration source which was located in the center of liquid xenon sphere [4], the light yield was found to be 14.7 photoelectrons/keVee. This large light yield allows the analysis threshold to be lowered sufficiently for sensitivity to low mass WIMPs. In order to achieve optimal sensitivity, the entire detector volume was used due to the difficulty of position reconstruction to determine the event location such a small number of p.e..

The energy spectrum for all events in the entire volume of the detector over a 5.6 ton·day exposure is shown in Fig. 3. To maximize the sensitivity at low energy, only three simple type of timing cut were applied to the raw data. In order to remove events caused by the tail of the scintillation light observed in high energetic gamma, beta, alpha, and muon interactions in the detector, events that occurred within 10 ms of the previous event are rejected. Events whose timing distribution has an RMS greater than 100 ns are also removed. The last and most significant cut is designed to remove events which produce light predominantly through Cherenkov emission, in particular the beta particle emitted in the decay of ^{40}K contamination in the PMT photocathode [5]. Events with more than 60 % of their PMT hits within the first 20 ns of the event window are removed as Cherenkov-like. Each reduction step of the data is shown in Fig. 3.

Since the energy calibration was performed by using 122 keV gamma rays, the nuclear-recoil equivalent energy ($E_{\rm NR}$) is determined by conversion from electron equivalent energy ($E_{\rm ee}$) using the scintillation efficiency, $\mathscr{L}_{\rm eff}$, for nuclear recoils relative to that of 122 keV gammas. We follow the treatment of the energy dependence of $\mathscr{L}_{\rm eff}$ and its uncertainty is the same as in Ref. [7]. In the $\mathscr{L}_{\rm eff}$ framework, though the absolute energy scale is determined at 122 keVee, dark matter signals are expected to appear at lower energies and the energy scale uncertainty was evaluated by the lower energy calibration samples the detector simulation at these lower energies. In the detector simulation the non-linearity response of liquid xenon scintillation light was taken into account base on [8, 9]. The apparent deviation of

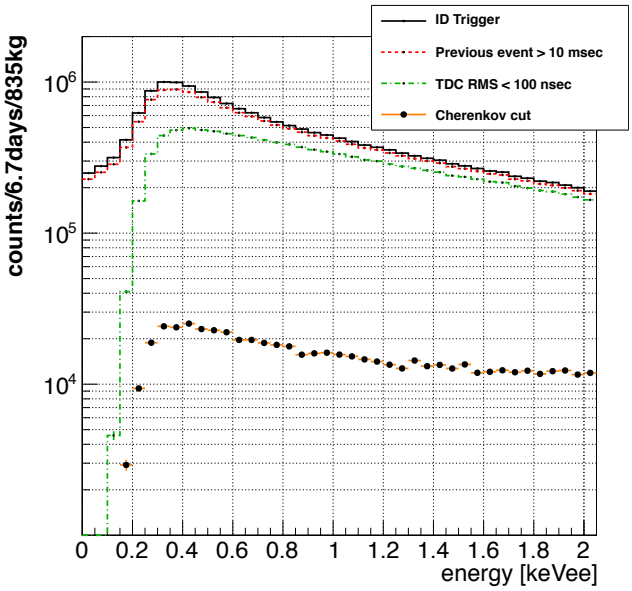

Fig. 3: The obtained energy spectrum at each reduction step of the data. Raw data is shown as the black solid line, the result of the 10 ms to the previous event timing cut appears as the red dashed line, and the green dash-dotted line shows the data after application of the timing distribution width cut. The filled points show the result of the Cherenkov event cut.

the simulation from the data reflects not only imperfection in the modeling of the detector environment but also the non-linear response of electron-mediated events in liquid xenon at very low energy below 10keVee [10]. In the procedure which includes the lowest energy of 5.9 keV X-ray from ^{55}Fe, the response at lower energies is extrapolated using a linear fit through all calibration energies. In the analysis the fitting error 1.3 % at 0.3 keVee, is treated as a systematic effect on the energy scale, however, the effect of this uncertainty is small relative to that induced by the uncertainty in $\mathscr{L}_{\rm eff}$, which is 13 % at the same energy. The expected WIMP acceptance efficiency of these cuts was estimated with the detector simulation. In the simulation WIMP recoil energy spectra were generated

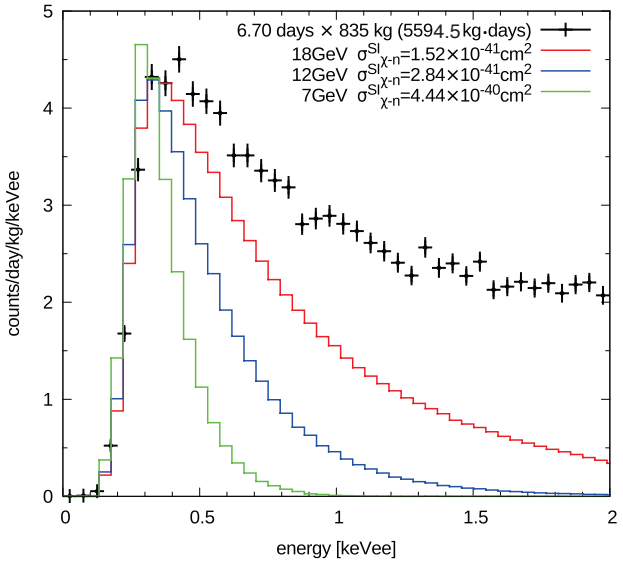

Fig. 4: Simulated WIMP energy spectra in the XMASS detector assuming the maximum cross section that provides a signal rate no larger than the observation in any bin above 0.3 keVee. WIMP mass of 7, 12, 18 GeV cases are shown. (from bottom to top in thin line)

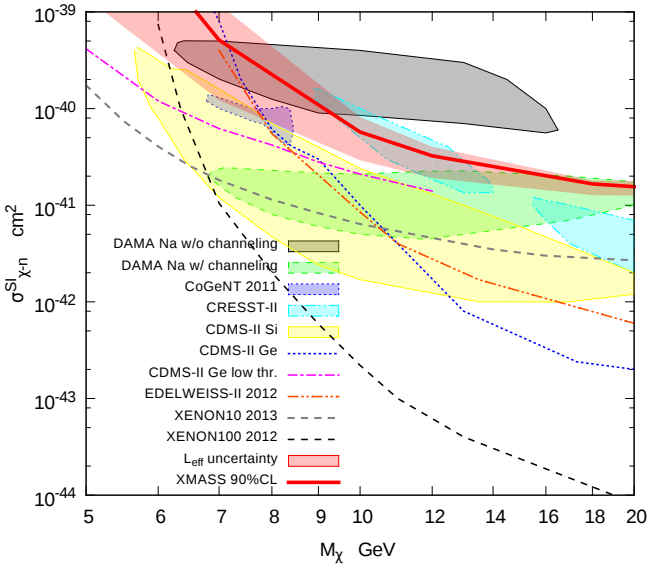

Fig. 5: Spin-independent elastic WIMP-nucleon cross section as a function of WIMP mass. All systematic uncertainties except that from $\mathscr{L}_{\rm eff}$ are taken into account in the XMASS 90 % C.L. limit line. The effect of the $\mathscr{L}_{\rm eff}$ uncertainty on the limit is shown in the band. Limits from other experiments and favored regions are also shown [15, 16, 17, 18, 19, 20, 21].

for each WIMP mass and MC events were distributed uniformly throughout the detector volume using a liquid scintillation decay constant of 25 ns [11]. The size of the error bars comes primarily from the systematic uncertainty in the xenon scintillation decay constant, 25 ± 1 ns, which is estimated based on the difference between the XMASS model [11] and the NEST simulation [12] based on Dawson et al. measurement [13]. A systematic error on the selection efficiency is determined based on the error resulting from a linear fit to the points in the figure.

4 Result and Conclusions

The differential energy spectrum of nuclear recoil by WIMP were calculated base on [14]. In Fig. 4, the simulated WIMPs energy spectra was shown together with the observed spectrum after the data reduction was applied. WIMPs are assumed to be distributed in an isothermal halo with $v_o = 220$ km/s, a galactic escape velocity of $v_{\rm esc} = 650$ km/s, and an average density of 0.3 GeV/cm^3. In order to set a conservative upper bound on the spin-independent WIMP-nucleon cross section, the cross section is derived not to exceed the observed one in any energy bin above 0.3 keVee. the resulting 90 % confidence level (C.L.) limit derived from this procedure is shown in Fig. 5. The impact of the uncertainty from $\mathscr{L}_{\rm eff}$ is large in this analysis, so its effect on the limit is shown separately as a band.

Detail study on background in the energy spectrum, we believe that most of them originate on the inner surface of the detector [4, 22]. These events are attributed to radioactive contamination in the aluminum seal of the PMT entrance windows, ^{14}C decays in the GORE-TEX® sheets between the PMTs and the copper support structure. On going refurbishment of XMASS detector to remove those background will achieve more than one order of magnitude better sensitivity on WIMP-nucleon scattering cross section and will be started in fall 2013.

Acknowledgment: We gratefully acknowledge the cooperation of Kamioka Mining and Smelt- ing Company. This work was supported by the Japanese Ministry of Edu- cation, Culture, Sports, Science and Technology, Grant-in-Aid for Scientific Research, and partially by the National Research Foundation of Korea Grant funded by the Korean Government (NRF-2011-220-C00006).

References

[1] Y. Suzuki, arXiv:hep-ph/0008296.
[2] K. Abe *et al.* (XMASS collaboration), Phys. Lett. B 724 (2013) 46, arXiv:1212.6153v1
[3] J. Beringer et al. (Particle Data Group), Phys. Rev. D86, 010001 (2012).
[4] K. Abe *et al.* (XMASS collaboration), Nucl. Instr. Meth. A 716 (2013) 78.
[5] K. Abe *et al.* (XMASS collaboration), Phys. Lett B 719 (2013) 78.
[6] S. Fukuda et al., Super-Kamiokande collaboration, Nucl. Instrum. Meth. A501 (2003) 418.
[7] E. Aprile et al., Phys. Rev. Lett. 107 131302 (2011).
[8] T. Doke et al., Technique and Application of Xenon Detectors (Xenon 01), proceedings of the international workshop, Tokyo Japan December 2001, pg. 17.
[9] M. Yamashita et al., Nucl. Instrum. Meth. A 535 (2004) 692
[10] E. Aprile et al., arXiv:1209.3658.
[11] K. Ueshima, Doctor thesis, 2010, University of Tokyo; K. Ueshima et al., Nucl. Instr. and Meth. A 659 (2011) 161.
[12] M. Szydagis et al., JINST 6 P10002 (2011); NEST (Noble Element Simulation Technique) http://nest.physics.ucdavis.edu/site/
[13] J. V. Dawson et al., Nucl. Instr. and Meth. A 545 (2005) 690.
[14] J.D. Lewin and P.F.Smith, Astroparticle Phys. 6 (1996) 87.
[15] R. Bernabei et al., Eur. Phys. J. C 56, (2008) 333; R. Bernabei et al., Eur. Phys. J. C 67, (2010) 39.
[16] C. E. Aalseth et al., Phys. Rev. Lett., 106 131301 (2011).
[17] G.Angloher et al., Eur. Phys. J. C 72 (2012) 1971.

[18] Z. Ahmed et al., Science 327, (2010) 1619; Z. Ahmed et al., Phys. Rev. Lett. 106 131302 (2011).; D. A. Bauer et al, arXiv:1304.4279v1
[19] E. Armengaud et al., Phys. Rev. D 86, 051701(R) (2012)
[20] J. Angle et al. arXiv:1104.3088v4; Phys. Review. Lett. 107 051301 (2011)
[21] E. Aprile et al., arXive:1207.5988; J. Angle et al., Phys. Rev. Lett. 107 051301 (2011).
[22] Y. Suzuki for the XMASS collaboration, Proceedings of the International Workshop on the Identification of Dark Matter, Chicago, USA, 23-27 July, 2012.